

# Nonlinearity Correction of Brain Perfusion SPECT Based on Permeability-Surface Area Product Model

Tatsuro Tsuchida, Yoshiharu Yonekura, Sadahiko Nishizawa, Norihiro Sadato, Nagara Tamaki, Toru Fujita, Yasuhiro Magata and Junji Konishi

Department of Nuclear Medicine, Kyoto University Faculty of Medicine, Kyoto; Department of Radiology and Biomedical Imaging Research Center, Fukui Medical School, Fukui, Japan

It is well known that many cerebral perfusion tracers underestimate cerebral blood flow in high flow range. A model has been proposed to correct nonlinear relationship of flow and uptake of the tracers that accounts for the permeability-surface area product (PS model). **Methods:** We examined 43 patients in this study. To test the feasibility of this method for  $^{123}\text{I}$ -IMP,  $^{99\text{m}}\text{Tc}$ -HMPAO and  $^{99\text{m}}\text{Tc}$ -ECD, radioactivity ratios of cerebral regions to cerebellum (C/Cr) on SPECT images were compared with those of rCBF (F/Fr) measured by PET using the  $^{15}\text{O}$   $\text{CO}_2$  steady-state method. Coefficients for correction in the PS model was estimated by the least squares method, and SPECT data were corrected using these coefficients. **Results:** Estimated PS value by this method was highest in IMP (116 ml/min/100 g) followed by ECD (66 ml/min/100 g) and HMPAO (46 ml/min/100 g). The corrected SPECT data demonstrated an excellent linear relationship, which was close to unity, with rCBF. **Conclusion:** These results indicate that the PS model can be used for nonlinearity correction of brain perfusion SPECT.

**Key Words:** permeability-surface area product; PET; SPECT; regional cerebral blood flow

**J Nucl Med 1996; 37:1237-1241**

In recent years, various cerebral perfusion tracers, including  $^{123}\text{I}$ -N-isopropyl-p-iodoamphetamine (IMP),  $^{99\text{m}}\text{Tc}$ -d,l-hexamethyl-propyleneamine oxime (HMPAO) and  $^{99\text{m}}\text{Tc}$ -ethyl-cysteinate dimer (ECD), have been introduced in clinical nuclear medicine as an indicator of regional cerebral blood flow (rCBF) measured by SPECT. Although these tracers move across the blood-brain barrier (BBB) efficiently and regional brain distribution essentially reflects rCBF, the significant underestimation of rCBF in the high flow regions has also been demonstrated (1,2). This underestimation is due to either the influence of backdiffusion (1) or relatively low tracer extraction (3).

To correct the nonlinearity of the brain SPECT counts and rCBF, Lassen et al. (4) proposed the linearization algorithm based on the backdiffusion model of HMPAO. However, it may not be appropriate to apply this method for the tracers with limited first-pass extraction such as ECD. We have previously proposed a model for the correction of nonlinearity (5) using the permeability-surface area (PS) product model (6,7). In this article, we examined the feasibility of this approach for the linearization correction of IMP, HMPAO and ECD brain SPECT images.

## MATERIALS AND METHODS

### Subjects

We selected 43 patients (35 men, 8 women; aged 33-63 yr) examined by both PET and SPECT cerebral perfusion studies. Thirty patients were in a chronic state of ischemic or hemorrhagic stroke and 13 had other neurological diseases, including Alzheimer's dementia (7 patients), vascular dementia (3 patients), Binswanger type dementia (1 patient) and brain tumors (2 patients). Dementia was diagnosed using standard criteria (8,9). No patient had structural lesions in the cerebellum.

IMP-SPECT was performed on 15 patients, HMPAO-SPECT on 20 and ECD-SPECT on 8. No patient received SPECT two or more times. A PET study was performed in all patients to measure quantitative rCBF using the  $^{15}\text{O}$   $\text{CO}_2$  steady-state method. Inter-examination intervals of SPECT and PET were within 2 wk.

### SPECT Tracers

Iodine-123-IMP (0.45 mg N-isopropyl-p-iodoamphetamine hydrochloride in 3 ml saline solution) was supplied commercially. Patients received 111 MBq IMP intravenously. To block the accumulation of free radioactive iodine in the thyroid gland, potassium iodine (30 mg/day) was given for 4 days starting on the day before the study.

Technetium-99m-HMPAO was prepared from a freeze-dried kit by the addition of 1110 MBq freshly eluted pertechnetate in 5 ml saline solution just prior to injection, and approximately 925 MBq HMPAO were administered intravenously.

Technetium-99m-ECD was also prepared from a commercially supplied kit. The ECD preparation kit consisted of two vials, one containing a sterile and nonpyrogenic lyophilized mixture and the other a liquid phosphate buffer. Three milliliters of normal saline were injected into the first vial to dissolve its contents. Technetium-99m generator eluant (1110 MBq) was injected into the second vial and 1.0 ml of the contents of the first vial was then transferred into the second vial. The mixture was allowed to stand at room temperature for 30 min, after which approximately 925 MBq ECD were injected.

### SPECT

A multidetector ring-type SPECT scanner, which provides three transaxial images with a slice interval of 30 mm was used. The spatial resolution was 12 mm FWHM in the center of the field of view, and the axial resolution was 23.5 mm FWHM (10). Two SPECT scans were obtained to acquire six slices of SPECT images at 15-mm intervals. Data acquisition began 5, 10 and 30 min after the administration of IMP, HMPAO and ECD, respectively. Scanning time was 15 min for IMP and 10 min for both HMPAO and ECD. We started data acquisition at different times for three

Received Feb. 23, 1995; revision accepted Oct. 8, 1995

For correspondence or reprints contact: Tatsuro Tsuchida, MD, Department of Radiology, Fukui Medical School, 23 Shimoaizuki, Matsuoka-cho, Yoshida-gun, Fukui, 910-11 Japan.

tracers because each time frame was determined to maximize image quality and to maximally reflect CBF information for each tracer. Each time sequence was used routinely in our institute. IMP is trapped in the lung first, then distributes brain gradually. To maximize the CBF information, we started data acquisition as soon as possible (5 min) after injection. HMPAO is trapped in the brain at first-pass and the distribution is fixed, whereas backdiffusion a few minutes after injection should be considered. Ten minutes after injection was considered to be enough time to end the backdiffusion. ECD is also trapped in the brain and fixed rapidly and there is less backdiffusion compared to HMPAO. For the ECD study, 30 min after injection was chosen to minimize radioactivity outside of the brain. The patient's head was positioned parallel to the canthomeatal line using a light beam on the patient's face to ensure uniform positioning for SPECT imaging. The SPECT images were reconstructed by a filtered backprojection algorithm using a ramp filter convoluted with a Butterworth filter (cutoff frequency 0.3, order 4). Attenuation correction was performed using elliptical fitting. Scatter correction was not performed. The final SPECT images covered the field of 21 cm in diameter with a 64 × 64 matrix.

### PET Study

Regional cerebral blood flow (rCBF) was measured by the <sup>15</sup>O-carbon dioxide (CO<sub>2</sub>) steady-state method (11) using a multislice PET scanner, (12,13). One scanner had four detector rings, each containing 192 bismuth germanate crystals, which allowed simultaneous acquisition of seven tomographic slices at 16-mm intervals. The spatial resolution of the reconstructed clinical PET images was 10 mm in FWHM at the center of the field of view and an axial of 12 mm. The other camera simultaneously acquires 15 slices with an interslice distance of 7 mm. The spatial resolution was 9 mm FWHM in the transaxial plane and 6.5 mm in the axial direction. On both PET scanners, prior to the emission measurements, tomographic transmission data (<sup>68</sup>Ge/<sup>68</sup>Ga) were obtained for photon attenuation correction. Tissue activity concentration in the images was cross-calibrated against the well counter using a cylindrical phantom filled with <sup>18</sup>F solution. The subject's head was immobilized with a headholder and positioned parallel to the canthomeatal line using a light beam. A small catheter was placed in the brachial artery for blood sampling. The subject wore a light, disposable plastic mask and nasal cannula for inhalation of <sup>15</sup>O gas produced by a small cyclotron. The steady-state inhalation method for <sup>15</sup>O-labeled CO<sub>2</sub> with 5-min data acquisition and intermittent arterial blood sampling was used to calculate rCBF.

### Permeability Surface Area Model

We have assumed that these tracers have no backdiffusion and the kinetics are based on the microsphere model. Therefore, regional activity of the tracers in the brain can be expressed as follows:

$$C = F \cdot E \int_0^T Ca(t) dt, \quad \text{Eq. 1}$$

where F is rCBF (ml/min/100 g brain), E is first-pass extraction, and Ca(t) is arterial input function (5). Based on the assumption of the uniform PS throughout the brain, E can be expressed as a function of F and PS (6):

$$E = 1 - \exp\left(\frac{-PS}{F}\right). \quad \text{Eq. 2}$$

From Equations 1 and 2, the SPECT count ratio to the reference region (C/Cr) can be expressed as a function of flow ratio (F/Fr) and PS as follows:

$$\frac{C}{Cr} = \frac{F}{Fr} \cdot \frac{1 - \exp\left(\frac{-PS}{F}\right)}{1 - \exp\left(\frac{-PS}{Fr}\right)}. \quad \text{Eq. 3}$$

This equation can be facilitated as

$$Y = \frac{X\left(1 - \beta\left(\frac{1}{X}\right)\right)}{1 - \beta}, \quad \text{Eq. 4}$$

where X = F/Fr, Y = C/Cr and  $\beta = \exp(-PS/Fr)$ .

### Data Analysis

Initially, original PET images were interpolated to construct the three-dimensional volumetric dataset, and we selected the slices that were closest to the corresponding SPECT images. After adjusting the pixel size, PET and SPECT images were superimposed visually by shifting and rotation. Identical regions of interest (ROIs) then were placed on the cerebral cortices, 17 × 17 mm in size, and cerebellar hemispheres, 23 × 23 mm in size. Relatively large ROIs were chosen to compensate for the different partial volume effects caused by the varying spatial resolution of PET and SPECT. ROIs were placed in the frontal, temporal, occipital and parietal cortices in the bilateral cerebral hemispheres. In cerebrovascular diseases, to exclude the effect of crossed cerebellar diaschisis or hypoperfusion (14,15), ROIs in the cerebellar hemisphere were placed ipsilateral to the cerebral lesion. The ratio of cerebral region-to-cerebellum on SPECT (Y) and PET (X) was compared. These datasets were used to estimate  $\beta$  in Equation 4. The optimal value of  $\beta$  was obtained with least-squares fitting methods.

The linearization correction of the relative SPECT counts (= C/Cr) was performed using the table look-up method because Equation 4 cannot directly provide X values from Y values. For this purpose, the look-up table of Y was calculated for each X value, and the relationship of X and Y was obtained by fourth-order polynomial curve fitting as follows:

$$X = A_0 + A_1Y + A_2Y^2 + A_3Y^3 + A_4Y^4. \quad \text{Eq. 5}$$

### RESULTS

Comparison of the SPECT and PET data demonstrated excellent correlation of tracer uptake and rCBF for all SPECT tracers as shown in Figure 1. However, the slope of the regression line was less than 45° for all tracers, suggesting lesser contrast between high- and low-flow regions in SPECT images compared with rCBF measured by PET. At the lower range of absolute values (F/Fr < 0.75), the uptake ratio C/Cr is consistently greater than the flow ratio, probably due to scatter radiation of the SPECT images, because scatter correction was not performed. Figure 1D shows the correlation between PET (F/Fr) and ECD (C/Cr) with fitting curve with  $\beta = 0.30$ , indicating that the fitting procedure worked well. Table 1 summarizes the calculated  $\beta$  and PS values for IMP, HMPAO and ECD. The obtained PS values were highest for IMP (116 ml/min/100 g), followed by ECD (66 ml/min/100 g) and HMPAO (46 ml/min/100 g). The values of A<sub>0</sub> to A<sub>4</sub> in Equation 5 were 0.07, 0.22, 1.75, -1.85, 0.97 on IMP, 0.02, 0.28, 1.21, -1.96, 1.45 on HMPAO and 0.11, 3.33, 1.75, -1.85, 0.97 on ECD. Figure 2 shows the comparison of uptake ratios and rCBF after linearization correction. In the linear regression analysis with corrected data, all SPECT tracers demonstrated excellent linear correlation, and the regression lines were close to the unity. Figure 3 demonstrates the ECD SPECT images before and after linearization. With linearization, image contrast of the lesion to normal cortex is more clear.

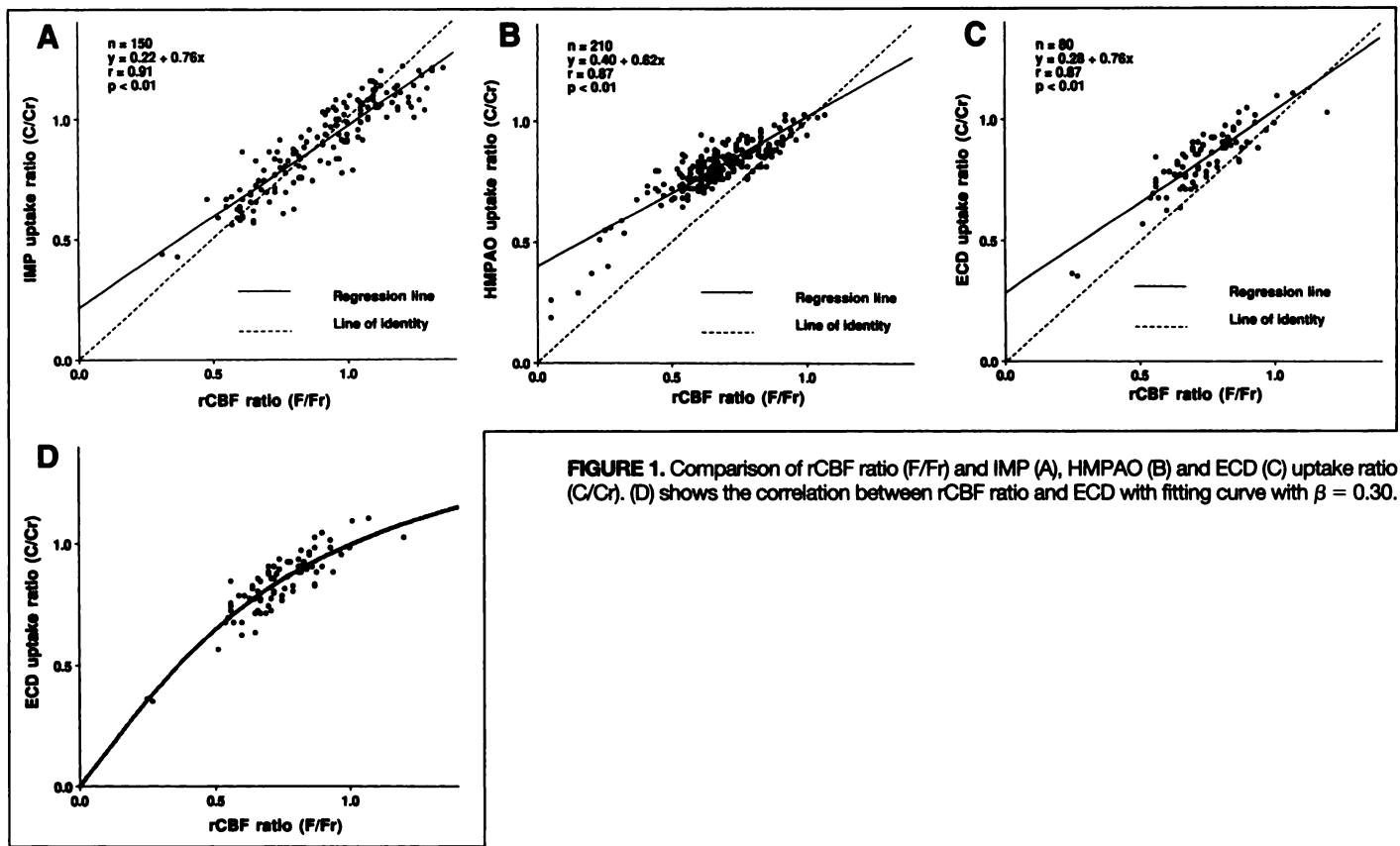


FIGURE 1. Comparison of rCBF ratio (F/Fr) and IMP (A), HMPAO (B) and ECD (C) uptake ratio (C/Cr). (D) shows the correlation between rCBF ratio and ECD with fitting curve with  $\beta = 0.30$ .

## DISCUSSION

It is well known that most of the cerebral perfusion tracers underestimate rCBF in the high flow range. This underestimation is due to the limited first-pass extraction of the tracer and/or backdiffusion from the brain to the blood. We previously reported that technetium-labeled SPECT tracers, such as HMPAO and ECD, are less favorable than IMP in regard to the

contrast between normal and hypoperfused regions (2), which may be due to the nonlinear relationship between rCBF and brain uptake of these tracers. For HMPAO, Lassen et al. (1,4) demonstrated that significant backdiffusion of lipophilic HMPAO was the major cause of the nonlinearity, although it showed sufficiently high first-pass extraction, and proposed a method for linearization correction. On the other hand, the first-pass extraction of ECD was reported to be lower than HMPAO or IMP (16,17). To correct the underestimation of rCBF by the limited extraction of the tracer, we proposed a correction method based on the PS product model (5).

The concept of PS product was originally proposed by Crone and Renkin (6,18). Our method is based on brain activity measured by SPECT, and the obtained PS values do not necessarily show the first-pass extraction. In the present results, the PS value for ECD was higher than that for HMPAO and lower than that for IMP. The PS value measured in human and

TABLE 1

Summary of  $\beta$ , Blood Flow in Reference Region and PS Values

	$\beta$	Fr (ml/min/100g)	PS value
IMP	0.11	52.7	116.3
HMPAO	0.43	54.5	46.0
ECD	0.30	55.0	66.2

Fr = blood flow in reference region.

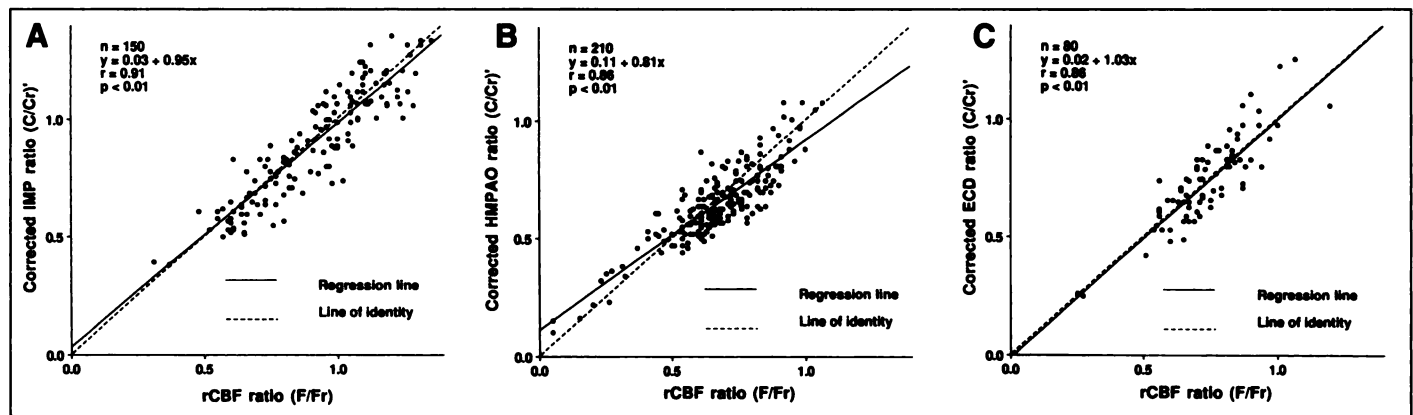
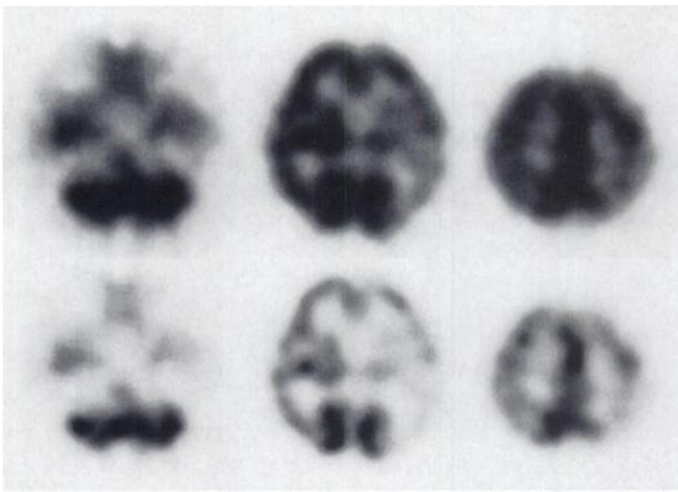


FIGURE 2. Comparison of F/Fr and IMP (A), HMPAO (B) and ECD (C) uptake ratio after correction with PS model (C/Cr)'. Excellent linear relationship was observed for each tracer.



**FIGURE 3.** ECD SPECT images before (upper) and after (lower) linearization. These images were normalized by each maximum value. A 63-yr-old man with left internal carotid artery occlusion showed decreased tracer uptake in the left occipito-parietal region. Clearer demonstration of the ischemic lesion after linearization is noted.

monkey's brains demonstrated the highest PS value for IMP, and the PS value of HMPAO is higher than that of ECD (19,20). IMP has first-pass extraction with slow washout (21–23), and the PS value in this study gave similar results as the monkey brain (19). The discrepancy for HMPAO and ECD is obviously due to the significant backdiffusion of HMPAO. On the other hand, ECD was reported to have lower extraction compared with HMPAO and IMP (3), with less backdiffusion than HMPAO (16), which suggests that this method may be the most suitable among the three tracers. Because the major reason for nonlinearity of HMPAO uptake and rCBF is tracer backdiffusion (4,24,25) and the slope of the regression line is far from unity in our study, it may not be appropriate to apply the present approach for linearity correction and the backdiffusion model may be more favorable (26,27).

Since the present approach is based on brain activity measured by SPECT, we must recognize that the PS value obtained in this study is determined by various factors, including first-pass extraction, backdiffusion and the physical characteristics of SPECT imaging. Hence, it is not a physiological PS value. For example, slow washout of IMP causes a significant decrease in brain activity at the end of scanning, which underestimates the PS value. Both limited spatial resolution and undesired scatter radiation decrease the contrast between high and low rCBF regions. Although we used  $^{15}\text{O}$  as a reference flow tracer, even it has limited extraction compared with  $^{11}\text{C}$  and  $^{15}\text{O}$ -butanol (7,28,29). Another issue is that physiological PS value differs across the brain (29), which was not implemented in our model. However, Berridge et al. (29) reported that the underestimation of rCBF by  $^{15}\text{O}$ -water compared to  $^{15}\text{O}$ -butanol in high flow ranges was well corrected using the uniform PS value, 133 ml/min/100 g. Hence, assumption of uniform PS value is at least practically helpful. Although the nonlinearity correction based on this model was successful for all three tracers, the PS values were estimated from group data; hence intersubject variation of the PS value was not taken into account. Our method may not be appropriate for the patient whose cerebellar flow decreased, such as bilateral cerebral infarction and spino-cerebellar degeneration.

Although this method has several limitations, it can be used widely for nonlinearity correction of clinical SPECT images by taking the advantage of its simplicity. For this purpose, it is necessary to validate the method in larger subject population

and with other different physiological and pathological conditions.

## CONCLUSION

The present approach based on the PS model may be useful for nonlinearity correction of brain perfusion SPECT images, especially for ECD.

## ACKNOWLEDGMENTS

We thank Hidenao Fukuyama, MD and Masatsune Ishikawa, MD, Kyoto University Hospital, for clinical assistance.

## REFERENCES

- Lassen NA, Andersen AR, Friberg H, Neirinckx RD. Technetium-99m-HMPAO as a tracer of cerebral blood flow distribution: a kinetic analysis [Abstract]. *J Cereb Blood Flow Metab* 1987;7:S535.
- Tsuchida T, Nishizawa S, Yonekura Y, et al. SPECT images of technetium-99m-ethyl cysteinate dimer in cerebrovascular diseases: comparison with other cerebral perfusion tracers and PET. *J Nucl Med* 1994;35:27–31.
- Walovitch RC, Hill TC, Garrity ST, et al. Characterization of technetium-99m-L-ECD for brain perfusion imaging: I. Pharmacology of technetium-99m-ECD in nonhuman primates. *J Nucl Med* 1989;30:1892–1901.
- Lassen NA, Andersen AR, Friberg L, Paulson OB. The retention of [ $^{99m}\text{Tc}$ ]-d,l-HMPAO in the human brain after intracarotid bolus injection: a kinetic analysis. *J Cereb Blood Flow Metab* 1988;8:S13–S22.
- Yonekura Y, Tsuchida T, Sadato N, et al. Brain perfusion SPECT with  $^{99m}\text{Tc}$ -bicisate: comparison with PET measurement and linearization based on permeability-surface area product model. *J Cereb Blood Flow Metab* 1994;14:S58–S65.
- Crone C. The permeability of capillaries in various organs as determined by use of the "indicator diffusion" method. *Acta Physiol Scand* 1963;58:292–305.
- Raichle ME, Eichling JO, Straatmann MG, Welch MJ, Larson KB, Ter-Pogossian MM. Blood-brain barrier permeability of  $^{11}\text{C}$ -labeled alcohol and  $^{15}\text{O}$ -labeled water. *Am J Physiol* 1976;230:543–552.
- Diagnostic and statistical manual of mental disorders*, 3rd ed. revised. American Psychiatric Association; 1987.
- Mckhann G, Drachmann D, Folstein M, et al. Clinical diagnosis of Alzheimer's disease: report of the NINCDS-ADRDA work group under the auspices of Department of Health and Human Services Task Force on Alzheimer's Disease. *Neurology* 1984;34:939–944.
- Yonekura Y, Fujita T, Nishizawa S, et al. Multidetector SPECT scanner for brain and body: system performance and applications. *J Comput Assist Tomogr* 1989;13:732–740.
- Frackowiak RS, Lenzi GL, Jones T, Heather JD. Quantitative measurement of regional cerebral blood flow and oxygen metabolism in man using  $^{15}\text{O}$  and positron emission tomography: theory, procedure and normal values. *J Comput Assist Tomogr* 1980;4:727–736.
- Senda M, Tamaki N, Yonekura Y, et al. Performance characteristics of Positologica III: a whole-body positron emission tomograph. *J Comput Assist Tomogr* 1985;9:940–946.
- Mukai T, Senda M, Yonekura Y, et al. System, design and performance of a newly developed high-resolution PET scanner using double wobbling mode [Abstract]. *J Nucl Med* 1988;29(suppl):877.
- Baron JC, Boussier MG, Comar D, Cattaigne P. Crossed cerebellar diaschisis in human supratentorial brain infarction. *Trans Am Neurol Assoc* 1980;105:459–461.
- Yamauchi H, Fukuyama H, Yamaguchi S, et al. Crossed cerebellar hypoperfusion in unilateral major cerebral artery occlusive disorders. *J Nucl Med* 1992;33:1632–1636.
- Murase K, Tanada S, Inoue T, et al. Kinetic behavior of  $^{99m}\text{Tc}$ -ECD in the human brain using compartment analysis and dynamic SPECT: comparison with  $^{99m}\text{Tc}$ -HMPAO [Abstract]. *J Nucl Med* 1992;33:909.
- Friberg L, Andersen AR, Lassen NA, Holm S, Dam M. Retention of  $^{99m}\text{Tc}$ -bicisate in the human brain after intracarotid injection. *J Cereb Blood Flow Metab* 1994;14:S19–S27.
- Renkin EM. Transport of potassium-42 from blood to tissue in isolated mammalian skeletal muscles. *Am J Physiol* 1959;197:1205–1210.
- Mathias CJ, Welch MJ, Lich L, Raichle ME, Volkert WA, Hung JC. Single-pass extraction of d,l and meso Tc-99m-HMPAO in primate brain [Abstract]. *J Nucl Med* 1988(suppl):29:747.
- Murase K, Tanada S, Inoue T, et al. Measurement of the blood-brain barrier permeability of [ $^{123}\text{I}$ ]-IMP,  $^{99m}\text{Tc}$ -HMPAO and  $^{99m}\text{Tc}$ -ECD in the human brain using compartment model analysis and dynamic SPECT [Abstract]. *J Nucl Med* 1991;32(suppl):911.
- Kuhl DE, Barrio JR, Huang SC, et al. Quantifying local cerebral blood flow by N-isopropyl-p-[ $^{123}\text{I}$ ]iodoamphetamine (IMP) tomography. *J Nucl Med* 1982;23:196–203.
- Winchell HS, Horst WD, Braun L, Oldendorf WH, Hattner R, Parker H. N-isopropyl-[ $^{123}\text{I}$ ]p-iodoamphetamine: single-pass brain uptake and washout; binding to brain synaptosomes; and localization in dog and monkey brain. *J Nucl Med* 1980;21:947–952.
- Yonekura Y, Nishizawa S, Mukai T, et al. Functional mapping of flow and backdiffusion rate of N-isopropyl-p-iodoamphetamine in human brain. *J Nucl Med* 1993;34:839–844.
- Andersen AR, Fruberg HH, Schmidt JF. Quantitative measurements of cerebral blood flow using SPECT and  $^{99m}\text{Tc}$ -d,l-HMPAO compared to xenon-133. *J Cereb Blood Flow Metab* 1988;8:S69–S81.

25. Murase K, Tanada S, Fujita H, Sakai S, Hamamoto K. Kinetic behavior of technetium-99m-HMPAO in the human brain and quantification of cerebral blood flow using dynamic SPECT. *J Nucl Med* 1992;33:135-143.
26. Inugami A, Kanno I, Uemura K, et al. Linearization correction of <sup>99m</sup>Tc-labeled hexamethyl-propyleneamine oxime (HMPAO) image in terms of regional CBF distribution: comparison to C<sup>15</sup>O<sub>2</sub> inhalation steady-state method measured by positron emission tomography. *J Cereb Blood Flow Metab* 1988;8:S52-S60.
27. Yonekura Y, Nishizawa S, Mukai T, et al. SPECT with <sup>99m</sup>Tc-d,l-hexamethyl-propyleneamine oxime (HMPAO) compared with regional cerebral blood flow measured by PET: effects of linearization. *J Cereb Blood Flow Metab* 1988;8:S82-S89.
28. Herscovitch P, Raichle ME, Kilbourn MR, Welch MJ. Positron emission tomographic measurement of cerebral blood flow and permeability-surface area product of water using [<sup>15</sup>O]water and [<sup>11</sup>C]butanol. *J Cereb Blood Flow Metab* 1987;7:527-542.
29. Berridge MS, Adler LP, Nelson AD, et al. Measurement of human cerebral blood flow with [<sup>15</sup>O]butanol and positron emission tomography. *J Cereb Blood Flow Metab* 1991;11:707-715.

## EDITORIAL

# Modeling Reality with Emission Tomography: What Is the Point?

In 1913, Niels Bohr presented his now familiar model of the atom, consisting of a central nucleus with "orbiting" electrons. We now know that this model does not accurately and fully represent reality. Indeed, quantum physicists such as David Bohm have argued that protons, neutrons and electrons do not actually exist as particles. Even so, we continue to use Bohr's model for many applications. Why? Because we can accomplish important goals by doing so. My mentor, Henry N. Wagner, Jr., often has said: "Be as rigorous as necessary, not as rigorous as possible."

Quantification is important in the practice of nuclear medicine. "Quantification" means more than assessment of the amount of radioactivity; it implies estimation of physiological or biochemical parameters of interest. Quantification involves a simplification or "filtering" of the raw data—an abstraction. Of necessity, this abstraction is based on a conceptual and associated mathematical model of the physiological or biochemical process. In practice, the need to model, and the utility of a particular model, depend on the model's intended purpose. That is, modeling can only be judged in the context of its usefulness in solving a specific research or clinical problem.

In this issue of *JNM*, Tsuchida et al. (1) describe the development and application of a model to correct the nonlinear relationship between regional cerebral blood flow (rCBF) and the uptake of [<sup>123</sup>I]IMP, <sup>99m</sup>Tc-HMPAO and <sup>99m</sup>Tc-ECD. I would like to make four points about modeling in emission tomography, the first three of which are illustrated by this excellent article. First, the success with which these investigators were able to produce corrected data with SPECT that correlated well with PET highlights

the advances SPECT has made. We now need to think in terms of "emission tomography" rather than distinguishing between SPECT and PET. This is true not only for "image quality" (e.g., spatial resolution, contrast or signal-to-noise ratio), but for estimation of physiological or biochemical parameters, such as rCBF (1) or even parameters as difficult to assess as receptor binding (2). Second, simplified approaches to kinetic modeling will promote more widespread use of modeling. These include easier acquisition protocols (e.g., the use of only a single dose or simplified blood sampling) and more automated data analyses (3-5). Third, since nuclear medicine is so oriented toward images, it seems likely that the type of quantification being discussed here will be presented in the form of images rather than as collections of numbers. Such images, called parametric images, have pixel values that represent a physiological or biochemical parameter rather than radioactivity concentration per se. They facilitate interpretation of regional data because they permit the viewer's brain to recognize regional patterns. For example, the bottom row of Tsuchida et al.'s Figure 3 shows model-corrected images that are no longer simple distributions of radioactivity, but have pixel values that are directly proportional to cerebral blood flow. These images are both more accurate and have higher contrast than the corresponding uncorrected images in the top row of the figure. Excellent additional examples of this point can be found in recent issues of *JNM* (4,6). A fourth point, not directly addressed by Tsuchida et al., is the concept of always judging utility in a specific context. The investigators do state that "it is necessary to validate the method in another group of subjects with a larger population and with different physiological and pathological conditions." Such a validation would demonstrate the quantitative accuracy of the model and their correction approach. I would argue that a completely different type of study would

be necessary to demonstrate the diagnostic or prognostic accuracy of their approach. Without such a study, we do not really know the clinical utility of the approach, although its advantages for research are clear. An excellent example of 'judgment of utility in context' is found in the January 1996 issue of *JNM* (7).

Few who use models believe that they are absolutely accurate descriptions of "reality" (however perceived) (8). They need not be in order to be useful. If we can clearly define a problem whose solution requires the ability to describe and (especially) predict the results of further measurements, and if a given model provides the relevant solution in a feasible way, it is useful, and its widespread application should be encouraged. The challenge is in articulating the degree of accuracy required and knowing when (to quote Dr. Wagner again) to "stop grooming the horse and start riding it."

Jonathan M. Links

The Johns Hopkins University  
Baltimore, Maryland

## REFERENCES

1. Tsuchida T, Yonekura Y, Nishizawa S, et al. Nonlinearity correction of brain perfusion SPECT based on permeability-surface area product model. *J Nucl Med* 1996;37:1207.
2. Westera G, Buck A, Burger C, Leenders KL, von Schulthess GK, Schubiger AP. Carbon-11- and iodine-123-labeled iomazenil: a direct PET-SPECT comparison. *Eur J Nucl Med* 1996;23:5-12.
3. Delforge J, Spelle L, Bendriem B, et al. Quantitation of benzodiazepine receptors in human brain using the partial saturation method. *J Nucl Med* 1996;37:5-11.
4. Petit-Taboue MC, Landeau B, Osmont A, Tillet I, Barre L, Baron JC. Estimation of neocortical serotonin-2 receptor binding potential by single-dose fluorine-18-setoperone kinetic PET data analysis. *J Nucl Med* 1996;37:95-104.
5. Onishi Y, Yonekura Y, Nishizawa S, et al. Noninvasive quantification of iodine-123-iomazenil SPECT. *J Nucl Med* 1996;37:374-378.
6. Zasadny KR, Wahl RL. Enhanced FDG-PET tumor imaging with correlation-coefficient filtered influx-constant images. *J Nucl Med* 1996;37:371-374.
7. Vera DR, Stadelnik RC, Metz CE, Pimstone NR. Diagnostic performance of a receptor-binding radiopharmacokinetic model. *J Nucl Med* 1996;37:160-164.
8. Wong DF, Gjedde A. Compartments and reaction volumes of brain fluid spaces: Shaken, not stirred [Editorial]. *J Nucl Med* 1996;37:126-127.

Received Feb. 28, 1996; revision accepted Jun. 6, 1996.

For correspondence or reprints contact: Jonathan M. Links, MD, Department of Radiation Health Sciences, The Johns Hopkins University, 615 N. Wolfe St., Baltimore, MD 21205.